Shin, H. and Santamarina, J. C. (2011) ***Géotechnique Letters*** **1**, 95–99, http://dx.doi.org/10.1680/geolett.11.00014

Open-mode discontinuities in soils

H. SHIN* and J. C. SANTAMARINA†

The formation of open-mode discontinuities is a common occurrence in soils. This family of discontinuities includes hydraulic fractures, gas-driven fractures, desiccation cracks, ice and hydrate lenses, and even roots. These discontinuities can be analysed at the particle scale or at the macroscale using constitutive models that are consistent with the effective stress-dependent behaviour of soils. Both analyses show that the medium is in compression everywhere and that growth is intimately related to unloading and expansion ahead of the tip. While these observations appear to be common to the development of all open-mode fractures in soils, there are pronounced invasion differences between miscible fluids and immiscible phases.

KEYWORDS: failure; numerical modelling; strain localisation

INTRODUCTION

The analysis of open-mode discontinuities in soils, such as hydraulic fractures and desiccation cracks, is typically based on concepts derived from equivalent-continuum fracture mechanics, sometimes adjusted to account for various aspects of soil behaviour. However, this approach fails to recognise the inherent particulate nature of soils. In this context, the concept of fracture formation in a fully fractured medium is not immediately obvious. Furthermore, an effective stress tensile failure is impossible in cohesionless granular materials, and total stress analyses do not contribute physical understanding to the process.

The mechanical analysis of open-mode discontinuities leads to an important first distinction pertaining to the miscibility of the invading fluid with the defending fluid that saturates the soil. Except for 'classical' hydraulic fracture, all the following examples refer to an immiscible invading phase (Fig. 1).

(*a*) Fractures driven by the invasion of a miscible fluid (Fig. 1(a)). This is the case of 'classical' hydraulic fractures in near-surface geotechnical applications, such as dams, where the invading fluid (e.g. water) is miscible with the saturating fluid (e.g. water). In general, these fractures develop normal to the least principal stress unless pronounced stratigraphic features play a dominant role (Bjerrum *et al.*, 1972; Jaworski *et al.*, 1981; de Pater *et al.*, 1994). Fluid leak-off normal to the fracture planes is proportional to the permeability of the medium.

(*b*) Fractures driven by the invasion of an immiscible fluid (Figs 1(b) and 1(c)). Gas invasion into water-saturated sediments or the forced invasion of water into oil-saturated reservoirs may cause open-mode discontinuities. There is no seepage or leak-off of the invading fluid into the formation normal to the fracture faces (end-member case) and the fracture advances normal to the minimum stress direction in homogeneous sediments.

(*c*) Desiccation cracks (Fig. 1(d)). This common surface phenomenon is a special case of invasion by an immiscible fluid, where air invades water-saturated sediment. Desiccation cracks typically nucleate at the surface (in homogeneous sediments) and propagate both laterally and vertically, forming vertical planes (Morris *et al.*, 1992; Konrad & Ayad, 1997; Rodriguez *et al.*, 2007; Thusyanthan *et al.*, 2007; Shin & Santamarina, 2011).

(*d*) Ice and methane hydrate lenses (Fig. 1(e)). The literature on frozen ground and the more recent publications on methane hydrate report extensively on ice and hydrate lenses found in fine-grained sediments. Ice lenses in near-surface frozen ground are temperature controlled and lenses align parallel to the isothermal front rather than normal to the minimum effective stress (Konrad & Morgenstern, 1981; O'Neill & Miller, 1985; Rempel, 2007). However, hydrate growth is gas-limited in most cases (i.e. sediments are already within the pressure–temperature stability field and hydrate grows as methane becomes available rather than being temperature controlled). In these conditions, it is anticipated that hydrate lenses tend to grow normal to the minor principal stress σ'_3; hydrate-bearing sediments are reviewed by Waite *et al.* (2009) and hydrate lens formation is discussed by Clennell *et al.* (1999).

(*e*) Roots: bio-mechanical optimisation (Fig. 1(f)). Root growth into granular materials resembles the propagation of an open-mode axisymmetric discontinuity, so one may wonder whether plants use similar strategies to optimally invade soils. Data show that the rate of elongation and the rate of radial expansion are related to mechanical conditions at the tip of the root: difficult invasion conditions promote radial expansion of the root before the root tip advances further into the 'weakened' soil mass ahead of the tip (Hettiaratchi *et al.*, 1990; Kirby & Bengough, 2002; Gregory, 2006).

(*f*) Others. Similar conditions develop at the tip of a penetrating cone (axisymmetric) or at the edge of a suction caisson or a sampler (quasi-planar).

The purpose of this letter is to identify tip mechanisms and processes that are compatible with the granular nature of soils and can explain common open-mode discontinuities.

Manuscript received 24 February 2011; first decision 14 April 2011; accepted 17 October 2011.
Published online at www.geotechniqueletters.com on 21 November 2011.
*School of Civil and Environmental Engineering, University of Ulsan, Ulsan, South Korea
†School of Civil and Environmental Engineering, Georgia Institute of Technology, Atlanta, GA, USA

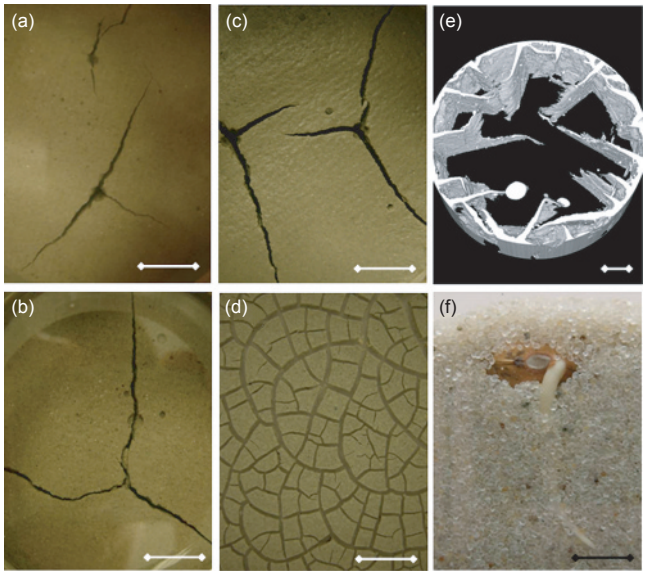

Fig. 1. Opening mode discontinuities in soils. Invading fluid is miscible with the saturating fluid: (a) classical hydraulic fracture. Invading phase is immiscible with the saturating fluid: (b) forced oil into a water-saturated sediment; (c) forced air into a water-saturated sediment; (d) desiccation cracks; (e) ice or hydrate lenses; (f) roots The segment superimposed on each picture is approximately 20 mm long. 3D tomogram of ice lenses in a frozen kaolin paste courtesy of G. Viggiani

A particle-level analysis and a macroscale effective stress numerical simulation follow.

PARTICLE-LEVEL ANALYSIS

Soil grains are displaced as open-mode discontinuities develop. This implies unbalanced particle-level forces. The forces most relevant to the examples listed earlier and order-of-magnitude estimates for a particle of diameter d are summarised in Table 1. Other particle-level forces, such as cementation and electrical forces, can be readily included.

The capillary pressure between immiscible fluids results from interfacial tension T_s and is inversely proportional to pore size r_{pore}, as predicted by Laplace's equation $\Delta u = 2T_s/r_{pore}$. The force due to capillarity C applies to vapour–water, gas–oil, oil–water, ice–water and hydrate–water systems where the host fluid is the wetting phase. (Note that ice and hydrate appear as solid phases in short timescales; however, their behaviour is that of an immiscible fluid in long timescales. Physical concepts and tabulated values can be found in Santamarina & Jang (2011).

Figure 2 shows schematic particle-level diagrams of open-mode discontinuities and anticipated particle-level forces induced by the invading phase. The two distinct conditions identified above are captured in the figure.

(*a*) Miscible invading fluid (Figs 2(a)–2(c)). Seepage-induced drag forces D accumulate away from the fracture wall. At the fracture wall, the drag forces must exceed particles' buoyant weight $D/B > 1$ to keep particles from falling off the fracture face; the seepage velocity required for equilibrium decreases with d^2 and this criterion is readily achieved in fine-grained sediments. The accumulation of the drag force into the soil mass must eventually exceed the far-field effective stress σ' to cause the fracture to open. Then, the fluid pressure inside the fracture u_{frac}, the fluid pressure in the far field u_{far} and the effective stress in the far field σ' must satisfy $u_{frac}/(\sigma' + u_{far}) > 1$.

(*b*) Immiscible invading phase (Figs 2(d)–(f)). Capillary C and root-induced forces R are imposed at the face of the discontinuity. Equilibrium conditions in terms of the driving capillary forces C or root-induced forces R and the internal skeletal forces N require the following conditions for the formation of open-mode discontinuities (forces are defined in Table 1).

(*i*) Ratio between capillary to skeletal forces: $C/N \approx 10T_s/(d\sigma') > 1$ for ice and hydrate lenses, desiccation cracks and gas-driven fractures. This condition is more readily satisfied in fine-grained sediments (small d) and at low effective stress σ'.

(*ii*) Ratio between root-induced and skeletal forces: $R/N = p_{tur}/\sigma' > 1$ for root growth, where the turgor pressure p_{tur} is the osmotic pressure inside the cell due to differences in concentration across the cell wall (the cell wall effect is included in p_{tur} for the sake of this mechanical analysis). Clearly, high effective stress hinders root growth. It should be noted here that the natural tendency for roots to grow downwards into higher effective stress conditions is gravity guided (i.e. gravitropism). Root growth may also respond to the availability of nutrients.

The particle-level visualisations in Fig. 2 show that the direction of particle-level forces causes expansion around the opening and that all particles are in compression everywhere, including at the tip, $N \geqslant 0$. High effective stress hinders the formation of open-mode discontinuities in all cases. Admittedly, the ratios identified earlier are

Table 1. Particle-level forces acting on a grain size d (see Santamarina (2003) for further details)

Force		Equation	Parameter; comments
N	Mean interparticle normal contact force acting on a particle that is part of a granular skeleton subjected to an effective stress σ'	$N = \sigma' d^2$	For grains arranged in simple cubic packing
B	Grain buoyant weight	$B = \frac{\pi}{6}(\gamma_m - \gamma_f)d^3$	γ_m = particle unit weight γ_f = fluid unit weight
D	Drag force on a particle moving in a fluid with a relative fluid–particle velocity v	$D = 3\pi\mu v d$	μ = fluid viscosity
R	Mean force a root can exert on a grain	$R = p_{tur} d^2$	p_{tur} = turgor pressure in the root
C	Maximum force due to capillarity exerted on a particle at the interface between the defending wetting fluid and the invading fluid	$C = \pi(2 + 2^{1/2})T_s d$	Based on Laplace's equation, $\Delta u = 2T_s/r_{pore}$, where T_s is the surface tension between fluids. The pore radius r_{pore} is geometrically related to grain size d

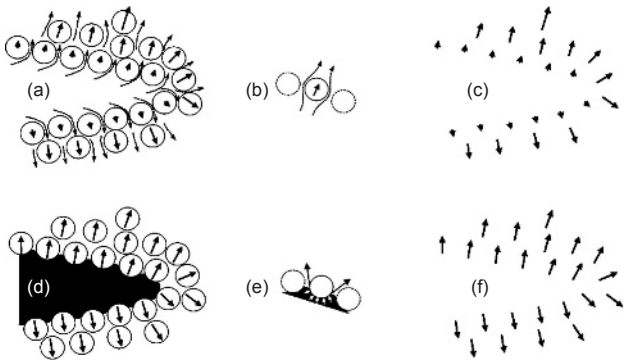

Fig. 2. Induced particle-level forces depend on the miscibility of the invading phase. Miscible fluid or typical 'hydraulic fracture': (a) the invading fluid permeates into the medium and (b) drags particles along its path; (c) drag-induced forces *D* accumulate away from the face of the fracture. Immiscible phase: (d) the advancing phase shown in black acts on the granular medium at the interface; (e) surface tension and pressure differences are responsible for the resulting particle force; (f) particle forces *C* or *R* induced at the interface between the invading and the defending fluid. In both cases, particles experience compressive forces everywhere; given these induced forces, unloading of skeletal forces and enlargement of voids is anticipated at the tip

first-order approximations; fabric, particle-scale variability, local arching and three-dimensional (3D) effects are not taken into consideration in this analysis.

EQUIVALENT CONTINUUM ANALYSIS

Let us consider an open-mode discontinuity developing in sediment under plane-strain conditions, subjected to an isotropic effective stress condition in the far field. The non-cohesive sediment is modelled as a modified cam clay material with Hvorslev and no-tension surfaces for the dry side. The stiffness tensor and stress updates are calculated using the consistent modulus formulation (Simo & Taylor, 1985) (model parameters and details are given in Fig. 3). For the case of an immiscible phase, the interfacial membrane prevents penetration and the invading fluid is represented as a capillary pressure applied against the sediment along the walls of the discontinuity. On the other hand, there is no interfacial membrane between miscible fluids; that is, the fluid pressure is the same on the fluid side as on the sediment side along the walls of the discontinuity, the far field is a drained boundary and a sudden increase in invading fluid pressure leads to a pressure transient until steady-state seepage conditions are attained and the sediment strains accordingly.

Figure 3(a) shows the medium subjected to an initial isotropic stress field of $\sigma'_0 = 100$ kPa. Then, the miscible fluid in the opening is pressurised to $u = 120$ kPa. The figure shows the mean effective stress at equilibrium and the evolution of q–p'–e conditions at selected locations. The effective stress is null around the face of the cavity and the fracture remains open because of the seepage forces. The effective stress increases into the wall as seepage forces transfer the drag onto the granular skeleton. There is volume expansion all around the cavity. However, the strain fields are very different (not shown in the figure): points along the fracture wall expand normal to the wall and there is almost no extension parallel to the wall; yet, points ahead of the tip experience a minor compression along the fracture direction and large extension normal to the fracture plane. In particular, it is noted that the strain normal to the flow direction is much greater at the tip than at the fracture wall (23 greater times in this simulation).

Figure 3(b) shows simulation results for the opening filled with an immiscible phase that exerts a normal pressure u_{im} against the walls of the discontinuity. We start the simulation with the invading phase at a pressure equal to the far-field isotropic effective stress $u_{im} = \sigma'_0 = 10$ kPa, so that the effective stress field is the same in all the sediment. Then, we increase the pressure in the immiscible phase gradually to $u_{im} = 14$ kPa while maintaining drained soil conditions. The resulting q–p'–e paths show an increase in effective stress and volume contraction on the fracture walls (point a) and unloading normal to the direction of propagation ahead of the tip, accompanied by an increase in void ratio (point b).

In both miscible and immiscible cases, the sediment is in compression everywhere, in agreement with the effective stress behaviour of cohesionless granular materials.

GROWTH–POSITIVE FEEDBACK

All the open-mode discontinuities analysed experience effective stress unloading and volume expansion ahead of the tip. This is a critical response to promote positive-feedback mechanisms that sustain the continuous localised growth of open-mode discontinuities in sediments.

Fractures caused by miscible fluids require the permeability to increase non-linearly with changes in porosity. Furthermore, based on a comprehensive numerical and analytical study, Shin & Santamarina (2010) concluded that pronounced anisotropic permeability develops at the tip in response to anisotropy in local strains.

Gas-driven fractures, desiccation cracks, ice and hydrate lenses, and roots grow as a result of the decrease in entry value (a generalisation of the air entry value concept) with an increase in porosity and pore size ahead of the tip during unloading and expansion. There are differences in the underlying growth processes. In desiccation cracks, the pressure difference between air and water $u_a - u_w$ develops as water evaporates while the air pressure remains constant. The evolution of lenses begins with ice or hydrate nucleation in the largest pores and crystal growth takes water from neighbouring pores (i.e. cryogenic suction) (Konrad & Morgenstern, 1981; Coussy, 2010). The turgor pressure inside a root is osmotic in nature and can exceed 0·7 MPa (see review in Gregory 2006); osmotic suction causes consolidation around the root, much like cryogenic suction.

In contrast to analyses based on standard fracture mechanics concepts, the effective stress compatible interpretation of open-mode discontinuities in granular materials (and the complementary particle-level mechanistic framework) can explain all known experimental observations (see Shin & Santamarina (2010, 2011) for examples).

CONCLUSIONS

Open-mode discontinuities in soils can result from the invasion of a miscible fluid (classical hydraulic fracture) or an immiscible phase (e.g. gas-driven fractures, desiccation cracks, ice and hydrate lenses, roots).

The regimes for these localisation events were identified using dimensionless ratios that capture the balance between controlling particle-level forces. The analysis confirms that open-mode discontinuities are facilitated in fine-grained sediments and low effective stress conditions.

The effective stress paths on the fracture walls are very different in miscible and immiscible invading phases. The effective stress tends to zero and the sediment on the fracture wall expands when the invading fluid is miscible with the saturating host fluid. However, sediment next to

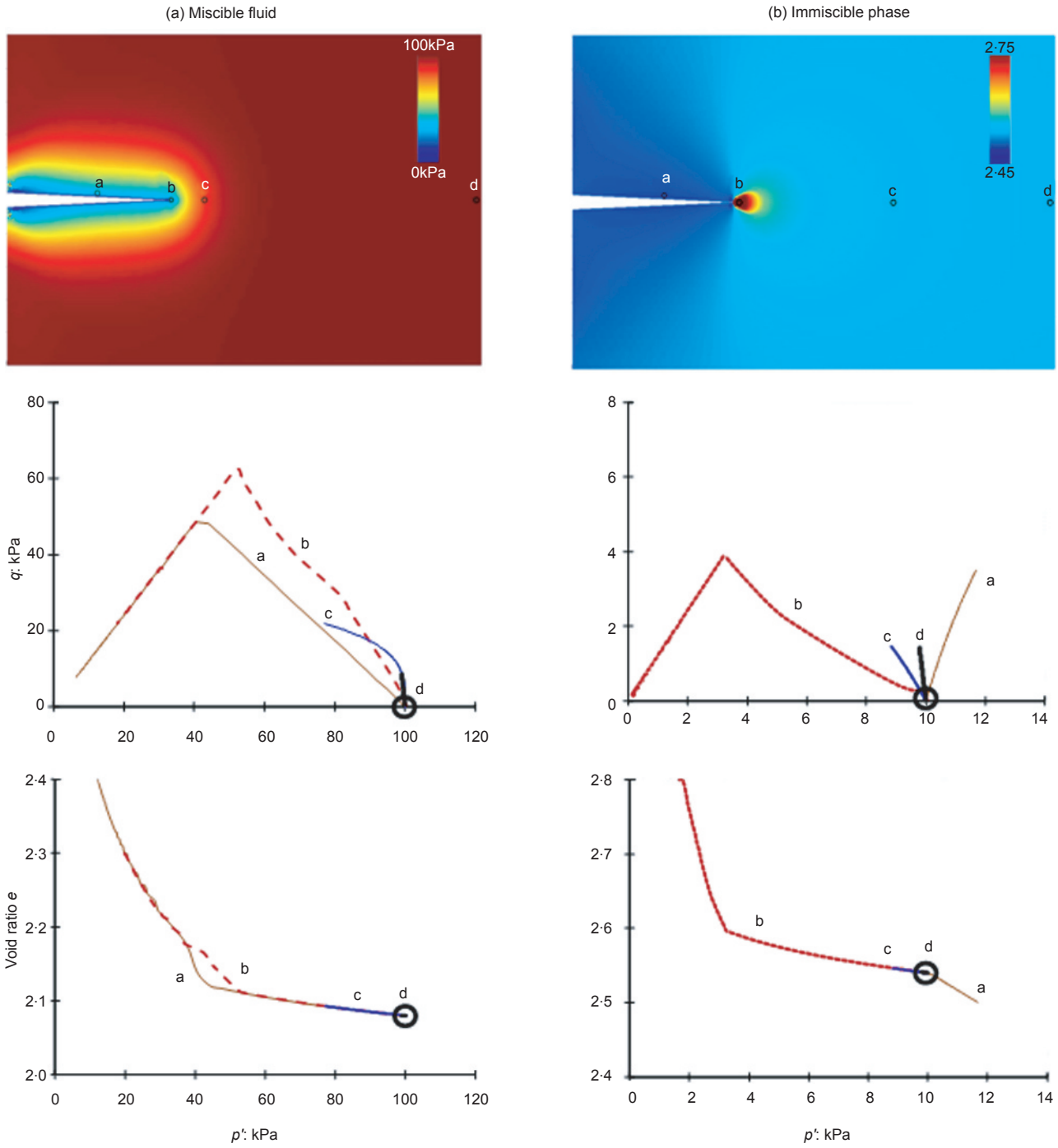

Fig. 3. Macroscale analysis – effective stress simulation using the modified cam clay model with tension cutoff (plane strain). (a) Miscible fluid: mean effective stress, q–p' and e–p' paths. (b) Immiscible phase: void ratio, q–p' and e–p' paths. The circles show the initial, isotropic stress condition for both cases. The constitutive model used is the modified cam clay model, adopting Hvorslev surface and tension cutoff and associated flow rule. Soil properties: normally consolidated sediment, compression index $C_c = 0{\cdot}46$, swelling index $C_s = 0{\cdot}15$, void ratio at 1 kPa $e_{1kPa} = 3$, failure stress ratio $M = 1{\cdot}2$, drained Poisson's ratio $\nu = 0{\cdot}3$. Element type: four nodes for fluid pressure and eight nodes for displacement. 2D plane strain. Constant σ' on the boundary

the walls experiences an increase in effective stress and consolidation takes place when the invading phase is immiscible.

Growth is intimately related to unloading and expansion ahead of the tip in all cases. A pronounced increase in local permeability associated with the anisotropic strains ahead of the tip sustains the propagation of miscible-fluid-driven fractures. Discontinuities caused by invading immiscible phases grow due to the lower normal stress, increased porosity and lower entry value that develop ahead of the tip.

Particle-level analyses and effective stress models show that sediments remain in compression everywhere, in agreement with the effective stress behaviour of cohesionless granular materials.

ACKNOWLEDGEMENTS

Support for this research was provided by the US Department of Energy and the Goizueta Foundation. We are grateful to Dr G. Viggiani at the Université Joseph Fourier in Grenoble for tomographic images of ice lenses in frozen soils. Thanks also go to C. Barrett for work on the manuscript.

REFERENCES

Bjerrum, L., Kennard, R. M., Gibson, R. E. & Nash, J. (1972). Hydraulic fracturing in field permeability testing. *Géotechnique* **22**, No. 2, 319–332.

Clennell, M. B., Hovland, M., Booth, J. S., Henry, P. & Winters, W. J. (1999). Formation of natural gas hydrates in marine sediments 1. Conceptual model of gas hydrate growth conditioned by host sediment properties. *J. Geophys. Res.* **104**, No. B10, 22985–23003.

Coussy, O. (2010). *Mechanics and physics of porous solids*. Chichester: Wiley.

de Pater, C. J., Cleary, M. P., Quinn, T. S., Barr, D. T., Johnson, D. E. & Weijers, L. (1994). Experimental verification of dimensional analysis for hydraulic fracturing. *SPE Prod. and Facil.* **9**, No. 4, 230–238.

Gregory, P. J. (2006). *Plant roots*. Oxford: Blackwell.

Hettiaratchi, D. R. P., Goss, M. J., Harris, J. A., Nye, P. H. & Smith, K. A. (1990). Soil compaction and plant-root growth. *Phil. Trans. Royal Soc. London Ser. B Biol. Sci.* **329**, No. 1255, 343–355.

Jaworski, G. W., Duncan, J. M. & Seed, H. B. (1981). Laboratory study of hydraulic fracturing. *J. Geotech. Eng. Div. ASCE* **107**, No. 6, 713–732.

Kirby, J. M. & Bengough, A. G. (2002). Influence of soil strength on root growth: experiments and analysis using a critical-state model. *Eur. J. Soil Sci.* **53**, No. 1, 119–127.

Konrad, J. M. & Ayad, R. (1997). An idealized framework for the analysis of cohesive soils undergoing desiccation. *Canad. Geotech. J.* **34**, No. 4, 477–488.

Konrad, J. M. & Morgenstern, N. R. (1981). The segregation potential of a freezing soil. *Canad. Geotech. J.* **18**, No. 4, 482–491.

Morris, P. H., Graham, J. & Williams, D. J. (1992). Cracking in drying soils. *Canad. Geotech. J.* **29**, No. 2, 263–277.

O'Neill, K. & Miller, R. D. (1985). Exploration of a rigid ice model of frost heave. *Water Resources Res.* **21**, No. 3, 281–296.

Rempel, A. W. (2007). Formation of ice lenses and frost heave. *J. Geophys. Res.* **112**, F02S21, http://dx.doi.org/10.1029/2006JF000525.

Rodriguez, R., Sanchez, M., Ledesma, A. & Lloret, A. (2007). Experimental and numerical analysis of desiccation of a mining waste. *Canad. Geotech. J.* **44**, No. 6, 644–658.

Santamarina, J. C. (2003). Soil behavior at the microscale: particle forces. In *Soil behavior and soft ground construction: the Ladd symposium, MIT, Boston, MA*. Reston, VA: ASCE, special publication 119, pp. 25–56.

Santamarina, J. C. & Jang, J. (2011). Energy geotechnology: implications of mixed fluid conditions. In *Proc. 5th Int. Conf. on Unsaturated Soils, Unsat 2010, Barcelona* (Alonso, E. E. & Gens, A. (eds)). London: Taylor & Francis Group, pp. 33 – 50.

Shin, H. & Santamarina, J. C. (2010). Fluid-driven fractures in uncemented sediments: underlying particle-level processes. *Earth Planet. Sci. Lett.* **299**, No. 1–2, 180–189.

Shin H. & Santamarina J. C. (2011). Desiccation cracks in saturated fine-grained soils: particle level phenomena and effective stress analysis. *Géotechnique* **61**, No. 11, 961–972.

Simo, J. C. & Taylor, R. L. (1985). Consistent tangent operators for rate-independent elastoplasticity. *Comput. Methods Appl. Mech. Eng.* **48**, No. 1, 101–118.

Thusyanthan, N. I., Take, W. A., Madabhushi, S. P. G. & Bolton, M. D. (2007). Crack initiation in clay observed in beam bending. *Géotechnique* **57**, No. 7, 581–594.

Waite, W. F., Santamarina, J. C., Cortes, D. D., Dugan, B., Espinoza, D. N., Germaine J. *et al*. (2009). Physical properties of hydrate-bearing sediments. *Rev. Geophys*. **47**, http://dx.doi.org/10.1029/2008RG000279.